1   **Active avoidance requires inhibitory signaling in the rodent prelimbic prefrontal cortex.**

2

3   **Authors & Affiliations**:

4   Maria M. Diehl[1], Christian Bravo-Rivera[1,2], Jose Rodríguez-Romaguera[3], Pablo A. Pagán-

5   Rivera[1], Anthony Burgos-Robles[4], Gregory J. Quirk[1,2]

6   [1]Department of Psychiatry, University of Puerto Rico School of Medicine, San Juan, PR 00936

7   [2]Department of Neurobiology & Anatomy, University of Puerto Rico School of Medicine, San

8   Juan, PR 00936

9   [3]Department of Psychiatry and Neuroscience Center, University of North Carolina at Chapel Hill,

10   Chapel Hill, NC 27599

11   [4]Department of Brain and Cognitive Sciences, Massachusetts Institute of Technology,

12   Cambridge, MA 02139

13   **Running Title**: Avoidance depends on prelimbic inhibitory responses.

14   **Corresponding Author**:

15   Maria M. Diehl

16   Department of Psychiatry and Neurobiology & Anatomy

17   University of Puerto Rico School of Medicine

18   San Juan, PR 00936

19   Tel: 787-999-3057

20   Email: maria.m.diehl@gmail.com

21   **Number of words in Abstract**: 150

22   **Number of words in Intro, Results, Discussion**: 4,067

23   **Keywords**: Fear, single unit recordings, optogenetics, channelrhodopsin, archaerhodopsin.

31   **Competing interests**: The authors declare that no competing interests exist.

32   **Abstract**

33   Much is known about the neural circuits of conditioned fear and its relevance to

34   understanding anxiety disorders, but less is known about other anxiety-related behaviors such

35   as active avoidance. Using a tone-signaled, platform-mediated active avoidance task, we

36   observed that pharmacological inactivation of the prelimbic prefrontal cortex (PL) delayed

37   initiation of avoidance. However, optogenetic silencing of PL neurons did not delay avoidance.

38   Consistent with this finding, inhibitory, but not excitatory, responses of rostral PL neurons to the

39   tone were correlated with initiation of avoidance. To oppose inhibitory responses, we

40   photoactivated rostral PL neurons during the tone to maintain pre-tone firing rate.

41   Photoactivation of rostral PL (but not caudal PL) neurons at 4 Hz (but not 2 Hz) delayed or

42   prevented avoidance. These findings suggest that the initiation of active avoidance requires

43   inhibitory neuronal responses in rostral PL, and underscores the importance of designing

44   behavioral optogenetic studies based on neuronal firing patterns.

45   **Introduction**

46   Core symptoms of post-traumatic stress disorder and other anxiety disorders include

47   excessive fear and maladaptive avoidance (DSM–V, 2013). The neural mechanisms of

48   excessive fear have been well-characterized in rodents using Pavlovian fear conditioning

49   (Johansen et al., 2011, Herry and Johansen, 2014, Giustino and Maren, 2015, Do Monte et al.,

50   2016), yet the neural underpinnings of active avoidance are just beginning to emerge. Previous

51   work in rats has shown that the prefrontal cortex, amygdala, and striatum are all necessary for

52   the expression of active avoidance (Martinez et al., 2013, Moscarello and LeDoux, 2013, Beck

53   et al., 2014, Jiao et al., 2015, LeDoux et al., 2017). Using a tone-signaled, platform-mediated

54   avoidance task, we previously observed that pharmacological inactivation of the prelimbic

55   prefrontal cortex (PL) impaired the expression of avoidance without affecting freezing (Bravo-

56   Rivera et al., 2014). Furthermore, avoidance that persisted following extinction training was

57   correlated with excessive PL activity, as indicated by the immediate early gene cFos (Bravo-

58   Rivera et al., 2015), suggesting that PL activity drives active avoidance.

59   Important questions remain, however, regarding the role of PL in avoidance. First, how

60   do PL neurons signal avoidance? Fear conditioning mainly induces excitatory responses to

61   conditioned tones in PL that correlate with freezing (Baeg et al., 2001, Burgos-Robles et al.,

62   2009, Sotres-Bayon et al., 2012, Isogawa et al., 2013, Pendyam et al., 2013, Chang et al.,

63   2010), but firing properties of PL neurons during active avoidance have not been previously

64   studied. In platform-mediated avoidance, PL signaling of avoidance may differ from PL signaling

65   of freezing or foraging for food (Burgos-Robles et al., 2013), both of which can interfere with

66   platform avoidance. Second, is PL activity correlated with the initial decision to avoid and/or the

67   subsequent expression of avoidance?

68   We addressed these questions with single unit recordings to determine PL signaling

69   during discrete events leading to the successful execution of active avoidance. We then

70   optogenetically silenced or activated PL neurons, based on the observed firing properties. We

71   find that inhibitory responses (rather than excitatory responses) of rostral PL neurons at tone

72   onset are correlated with the initiation of active avoidance. Reducing these inhibitory neuronal

73   responses with photoactivation delayed or prevented the initiation of avoidance, suggesting that

74   prefrontal inhibition underlies the decision to avoid danger.

75

76   **Results**

77   **Pharmacological inactivation of PL delays the initiation of avoidance.**

78   We first replicated prior findings that pharmacological inactivation of PL with muscimol

79   (MUS) impairs avoidance in this task (Bravo-Rivera et al., 2014), with two modifications: 1) we

80   used fluorescently labeled MUS to assess spread to adjacent regions, and 2) we analyzed the

81   time course of avoidance behavior across the 30 sec tone cue. Because the 2 sec shock co-

82   terminates with the tone, the rat has 28 sec to stop pressing the lever for food and step onto the

83   platform to escape the shock. Furthermore, in this task, avoidance comes at a cost, as it

84   competes with access to food. Thus, the involvement of PL could vary with changes in the cost

85   and/or urgency of avoidance as the tone progresses (Zeeb et al., 2015, Hosking et al., 2016).

86   Histological analysis showed that MUS was confined to PL in its mid rostral-caudal

87   extent (Figure 1A). Rats showing substantial spread to adjacent infralimbic cortex were

88   excluded (n=3). In some cases, MUS reached the ventral half of cingulate cortex (Cg1), but they

89   were included due to similar functions of Cg1 and PL (Courtin et al., 2014). Following surgical

90   implantation of cannulas, rats were trained in platform-mediated avoidance over 10 days as

91   previously described (Figure 1B, Bravo-Rivera et al., 2014, Rodriguez-Romaguera et al., 2016).

92   At Test 1 (Day 11), we infused MUS into PL at the same concentration as our prior studies

93   using fluorescent MUS (Do-Monte et al., 2015b, Rodriguez-Romaguera et al., 2016) and waited

94   45 minutes before commencing a 2-tone test of avoidance expression (without shock). Figure

95   1C shows that MUS inactivation significantly reduced the time spent on the platform during the

96   tone, as compared to saline (SAL) infused controls (SAL 92% vs. MUS 57%, unpaired t-test,

97    $t_{(28)}$=-4.019, p<0.01, Bonferroni corrected). An analysis of avoidance across the tone in 3 sec

98   bins (Figure 1D) indicated that 11/13 MUS-infused rats were significantly delayed in their

99   initiation of avoidance (repeated measures ANOVA, $F_{(1,9)}$=4.076, p<0.001; post hoc Tukey test,

100   0-15 sec **p<0.01, 15-21 sec *p<0.05), and 2/13 rats never avoided (Mann Whitney U Test,

101   p<0.001, Figure 1E). MUS also increased freezing during the tone (Figure 1E inset; SAL = 36%

102   vs. MUS = 55% freezing, unpaired t-test, $t_{(28)}$=2.460, p=0.020). MUS inactivation of PL had no

103   effect on locomotion, as indicated by distance traveled in an open field test during a 5 min

104   period (SAL n=10, 13.23 m vs. MUS n=10, 12.53 m, unpaired t-test, p=0.614). Nor did it affect

105   anxiety levels, as both groups spent a similar amount of time in the center of the open field (SAL

106   = 15.69 sec vs. MUS = 18.76 sec, unpaired t-test, p=0.363). Thus, in the majority of rats,

107   pharmacological inactivation of PL slowed the initiation of avoidance during the tone.

108

109   **Photosilencing of PL neurons does not delay avoidance.**

110   Because pharmacological inactivation of PL delayed avoidance initiation, we reasoned

111   that tone-induced activity in PL would be essential for early avoidance. To asses this, we used

112   an optogenetic approach, expressing the microbial opsin archaerhodopsin (Arch) in PL, which

113   causes a hydrogen proton efflux to hyperpolarize neurons when exposed to 532 nm (green)

114   light (Chow et al., 2010, Han et al., 2011). We delivered Arch by infusing an adeno-associated

115   virus (AAV) encoding both Arch and enhanced yellow fluorescent protein (eYFP) under the

116   control of the CAMkII-α promotor to target glutamatergic projection neurons

117   (AAV5:CaMKIIα::eArchT3.0-eYFP; Liu and Jones, 1996). We first confirmed that Arch silences

118   PL neurons in anesthetized rats by recording extracellular activity in PL while illuminating Arch-

119   expressing PL neurons (Figure 2A). Laser illumination significantly decreased the firing rate of

120   41/70 neurons, and increased the firing rate of 11/70 neurons (Figure 2A, paired t-tests

121   comparing pre-laser vs laser activity of each unit using 1-sec time bins, all p's<0.05).

122   Next, we infused Arch into PL, distinguishing between rostral PL (rPL; defined as dorsal

123   to medial orbitofrontal cortex and anterior to the infralimbic cortex) and caudal PL (cPL; defined

124   as dorsal to the infralimbic cortex; Figure 2B) based on distinct connectivity of these sub-regions

125   (Floyd et al., 2000, Floyd et al., 2001). Ten days of avoidance training commenced 6-8 weeks

126   after viral infusion. Rats were then tested for avoidance expression. PL neurons were

127   illuminated with laser during the first tone, followed by a second tone with the laser off.

128   Surprisingly, avoidance initiation was not impaired by photosilencing of either rPL (Figure 2C) or

129   cPL (Figure 2D&F). Further examination showed that photosilencing rPL neurons had no

130   significant effect on the time course of avoidance following tone onset (Figure 2E left). However,

131   rPL-Arch rats avoided significantly earlier compared to rPL-eYFP control rats, as measured by

132   avoidance latency (Figure 2E right, Mann Whitney U test, p=0.0202).

133   The lack of impairment of avoidance may suggest that we failed to sufficiently inhibit PL

134   activity via Arch photosilencing. Arguing against this, however, photosilencing rPL neurons

135   during early avoidance training (on day 2) significantly reduced tone-induced freezing (eYFP-

136   control, n=9, 31% vs. eYFP-Arch n=8, 7% freezing, unpaired t-test, $t_{(15)}$=0.288, p=0.0115). Thus,

137   contrary to our initial hypothesis, excitatory activity of PL projection neurons does not appear to

138   be necessary for initiation of avoidance. Instead, silencing rPL tended to facilitate avoidance (as

139   indicated by the decrease in latency), raising the possibility that avoidance signaling may

140   involve rPL inhibition rather than excitation.

141

142   **Inhibitory responses in rostral PL neurons correlate with the initiation of avoidance.**

143   An assumption of our photosilencing approach was that increased activity in PL neurons

144   is correlated with avoidance, however, this hypothesis had never been tested. We therefore

145   performed extracellular single unit recordings in PL of well-trained rats during avoidance

146   expression. Units were recorded from the full rostral-caudal extent of PL (Figure 3A). We first

147   characterized PL activity at tone onset (Figure 3B-D). Both excitatory and inhibitory responses

148   were observed at tone onset (Figure 2B right). Figure 3C shows the proportions of neurons that

149   were significantly responsive (at each 500 ms bin) throughout the tone. Out of a total of 241

150   neurons, 34 were excited (14%, $Z > 2.58$ ($p<0.01$) in the first 500 ms) and 25 were inhibited

151   (10%, $Z < -1.96$ ($p<0.05$) in the first or second 500 ms bin) at tone onset, relative to 10 sec of

152   pre-tone activity (Figure 3D left). This brief post-tone latency (<1 sec) was selected to ensure

153   that the activity of PL neurons was limited to the tone, and not subsequent behavior, such as

154   platform entry, which typically occurred ~5 sec after tone onset (see black dots above graph in

155   Figure 3C).

156   To determine if these tone responses were correlated with avoidance, rather than

157   sensory perception of the tone, we compared PL responses in this group of rats with those of a

158   naïve control group trained to press for food and presented with tones in the same chamber with

159   the platform. Naïve rats were free to mount the platform and explore the chamber, but were

160   never shocked. To determine whether activity at tone onset might represent the aversiveness of

161   the tone, we also compared responses in avoidance rats with responses in rats subjected to

162   auditory fear conditioning in the same chamber (re-analysis of data from Burgos-Robles et al.,

163   2009). Surprisingly, there were no significant differences in the percentage of neurons showing

164   excitatory tone responses in the avoidance group compared to the naïve or fear groups (Figure

165   3D right; avoidance-trained: 34/241 (14%), naïve: 20/166 (12%), fear: 25/191 (13%), Chi Square

166   = 0.242, p=0.886). Inhibitory responses, however, occurred more frequently in avoidance-

167   trained rats compared to naïve or fear rats (avoidance-trained: 25/241 (10%), naïve: 3/166 (2%),

168   fear: 3/191 (2%), Chi Square = 22.649, p<0.001).

169   We then compared tone responses in avoidance and naïve rats at multiple time points

170   around the tone onset. Consistent with the data shown in the pie charts of the avoidance and

171   naïve groups, the percentage of excited cells did not significantly differ between avoidance

172   (gold) and naïve (light yellow) rats at tone onset (time = 0 sec, Figure 3D bottom). The

173   percentage of inhibited cells, however, was significantly higher in avoidance rats compared to

174   naïve rats during the first two 500 ms bins (Fisher Exact tests, both p's<0.01). Group differences

175   observed after tone onset for both excitatory and inhibitory responses likely reflect the

176   expression of avoidance behavior, which occurred in the avoidance group but not the naïve

177   group.

178   We next examined PL activity at platform entry, defined as the moment at which the rat's

179   head entered the platform zone (Figure 3E-G). Activity around platform entry was compared to

180   the same pre-tone baseline used in assessing responses to tone onset. Both excitatory and

181   inhibitory responses to platform entry were observed (Figure 3E right). Figure 3F shows the

182   proportion of neurons that were responsive at each 500 ms time bin around platform entry. PL

183   neurons were either excited (n=40/218; 18%; Z > 2.58 in the first 500 ms) or inhibited (22/218;

184   10%; Z < -1.96 in the first or second 500 ms bin) at platform entry (Figure 3G left). The

185   proportions showing each response in avoidance-trained rats did not differ significantly from

186   those in naïve controls (Figure 3G right; n=23/160; 15% excited; n=10/160; 6% inhibited, Fisher

187   Exact Tests, excited p=0.331; inhibited p=0.197), suggesting that platform entry responses in

188   PL represent sensory perception and/or motor responses rather than avoidance of threat (Amir

189   et al., 2015). Only inhibitory responses at tone onset correlated with initiation of avoidance of

190   threat.

191   We then compared platform entry responses in avoidance and naïve rats at multiple time

192   points around platform entry. Similar to tone responses, the percentage of excited cells did not

193   significantly differ between avoidance (gold) and naïve (light yellow) rats at platform entry (time

194   = 0 sec, Figure 3G bottom). Nor did the percentage of inhibited cells significantly differ at most

195   time points (Fisher exact test), suggesting that activity changes at platform entry do not reflect

196   avoidance of threat. Group differences observed after platform entry likely reflect sustained tone

197   responses in avoidance rats, which were not present in naïve rats, as they mounted the platform

198   outside of the tone.

199   In order to determine whether platform entry responses were distinct from tone

200   responses, we examined activity during platform entry only in the neurons that showed tone

201   responses (Figure 3H). Of the 34 cells that were excited at tone onset, only 7 (20%) were also

202   excited at platform entry. Similarly, of the 25 cells that were inhibited at tone onset, only 9 (36%)

203   were also inhibited at platform entry. Figure 3H shows the average normalized response (Z-

204   score) of excited or inhibited responses at tone onset, followed by their responses at platform

205   entry. This demonstrates that neurons exhibiting platform entry responses are largely distinct

206   from those exhibiting tone onset responses. Taken together, these results show that initiation of

207   avoidance is correlated with inhibitory responses in PL at tone onset but not with excitatory or

208   inhibitory responses at platform entry.

209   Further characterization of inhibitory tone responses in PL revealed that most inhibitory

210   responses (n=20/25) were not sustained 15 sec after tone onset, whereas 20% (n=5/25) were

211   sustained throughout the tone (Figure 4A). Inhibition reduced the firing rate from an average of

212   6Hz to 2 Hz within 1 sec after tone onset (Figure 4B). The majority of neurons showing inhibitory

213   tone responses were located in rPL (blue, n=22/25) rather than cPL (Figure 4C; purple; n=3/25,

214   Fisher Exact Test, p=0.0383) and were likely putative projection neurons, based on their spike

215   width and baseline firing rate (> 225 µs, <15 Hz for PL) as shown in Figure 4D (for method, see

216   Sotres-Bayon et al., 2012). These results suggest that inhibition of rPL projection neurons at

217   tone onset signals the initiation of active avoidance.

218

219   **Countering inhibitory responses in rostral PL neurons delays or prevents avoidance.**

220   Our recording data demonstrate that inhibitory tone responses in rPL correlate with

221   initiation of avoidance. Because inhibited neurons decreased their firing rate from 6 Hz to 2 Hz

222   on average (Figure 4B), we reasoned that opposing this decrease should impair initiation of

223   avoidance. To oppose inhibition, we used channelrhodopsin (ChR2) targeting CAMkIIα-positive

224   neurons to activate rPL neurons at 4 Hz, concurrent with the tone. To confirm our method, we

225   first measured extracellular unit activity in anesthetized rats from ChR2-expressing rPL neurons

226   exposed to blue light (473nm) illumination (Figure 5A). Figure 5B shows a representative rPL

227   neuron increasing its firing rate to 4 Hz photoactivation. We found that 4 Hz photoactivation

228   increased the firing rate in 38% of the neurons and decreased the firing rate in 24% of neurons

229   (Figure 4C left; n=112, 4 Hz, 30 sec duration, 5 ms pulse width, 8-10 mW illumination, student's

230   t-test, p<0.05). Photoactivation at 4 Hz increased firing rate from 1.41 Hz to 3.34 Hz on average,

231   in neurons that were significantly excited (Figure 4C right). We found that photoactivation at 2Hz

232   increased the firing rate in 46% and decreased the firing rate of 34% of neurons (Figure 4E left;

233   n=76, 2 Hz, 30 sec duration, 5 ms pulse width, 8-10 mW illumination, student's t-test, p<0.05).

234   Photoactivation at 2 Hz increased firing rate from 0.4 Hz to 1.16 Hz on average, in neurons that

235   were significantly excited (Figure 4E right). As expected, 2 Hz photoactivation had a weaker

236   effect than 4Hz activation on driving spiking activity in rPL neurons.

237   We next infused ChR2 into either the rPL or cPL and began avoidance conditioning 3-4

238   weeks after AAV infusion (Figure 6A). Following 10 days of avoidance training, rats were

239   exposed to two tones presented in the absence of shock. PL neurons were illuminated

240   throughout the first tone (4 Hz, 30 sec), followed by the second tone with the laser off.

241   Photoactivation of rPL neurons at 4 Hz markedly reduced avoidance expression as reflected in

242   the total time spent on the platform during the tone (Figure 6B; eYFP-control, n=9, 87% vs.

243   eYFP-ChR2, n=14, 27%, unpaired t-test, $t_{(21)}$=-4.779, p<0.001, Bonferroni corrected). In contrast

244   to rPL, photoactivation of cPL had no effect on avoidance (Figure 6C&E).

245   A closer examination of the time course of avoidance showed that photoactivation of rPL

246   significantly reduced avoidance throughout the tone (Figure 6D left; repeated measures

247   ANOVA, main effect (Group), $F_{(1)}$=18.642, p<0.001, interaction effect (GroupxBins) $F_{(9)}$=1.156,

248   p=0.326, post hoc Tukey test, last 9 3-sec bins, all p's<0.01). Photoactivation increased the

249   latency to avoid in 7/14 rats, and blocked avoidance entirely in 7/14 rats (Figure 6D right; Mann

250   Whitney U test, p<0.001), but it did not affect freezing (Figure 6D inset; eYFP-control 9% vs

251   eYFP-ChR2 14% time freezing, unpaired t-test, p=0.275). Reducing the rate of photoactivation

252   to 2Hz in rPL eliminated the effects on time course and latency of avoidance (Figure 6F).

253   Furthermore, shifting the 30 sec of 4 Hz photoactivation to the inter-tone interval did not impair

254   avoidance (Figure 6G). Thus, the photostimulation-induced impairment of avoidance showed

255   specificity with respect to location, time, and frequency. Finally, reducing the duration of 4 Hz

256   photoactivation from 30 sec to the first 15 sec of the tone delayed, but did not prevent,

257   avoidance as indicated by time on platform (Figure 6H left; Mann Whitney U test, p's<0.05 at 9-

258   15 sec) and avoidance latency (Figure 6H right, unpaired t-test, $t_{(17)}$=3.363, p=0.0037).

259   Photoactivation of rPL at 4 Hz had no effect on locomotion, as indicated by distance traveled in

260   an open field test during a 30 sec period (eYFP-control n=11, 2.71 m vs. eYFP-ChR2, n=15,

261   2.25 m, unpaired t-test, p=0.356). Nor did it affect anxiety levels, as both groups spent a similar

262   amount of time in the center of the open field (eYFP-control = 2.6727 sec vs. eYFP-ChR2 =

263   2.6733 sec, unpaired t-test, p=0.999). These findings are consistent with the hypothesis that

264   initiation of avoidance depends on tone-induced inhibition in rPL neurons.

265

266   **Discussion**

267   We investigated the neural mechanisms of the initiation of active avoidance. Whereas

268   pharmacological inactivation of PL delayed initiation of avoidance, optogenetic silencing did not.

269   Single-unit recordings revealed that initiation of avoidance was correlated with inhibitory, rather

270   than excitatory, tone responses of rostral PL neurons. Consistent with this, optogenetically

271   activating rPL neurons to oppose tone-induced inhibition delayed or prevented the initiation of

272   avoidance. These findings add to the growing body of evidence showing that inhibition within PL

273   is key for conditioned behavior (Ehrlich et al., 2009, Ciocchi et al., 2010, Sotres-Bayon et al.,

274   2012, Sparta et al., 2014) and highlight the importance of using in vivo recordings to guide

275   optogenetic manipulations of behavior.

276   Our findings extend previous findings that PL activity is necessary for avoidance

277   expression (Bravo-Rivera et al., 2014) by showing that PL processing contributes more to early,

278   rather than late, avoidance. Our findings appear to be at odds with prior cFos studies, showing

279   that the expression of active avoidance is correlated with increased activity in PL (Martinez et

280   al., 2013, Bravo-Rivera et al., 2015). Importantly, the excitatory responses we observed in PL

281   neurons were associated with either sensory correlates of the tone, or motor correlates of

282   platform entry, compared to naïve controls. Thus, previously observed increases in cFos

283   expression may represent sensory and/or motor features of avoidance-like behavior rather than

284   avoidance itself, which was correlated only with inhibitory responses in PL. This resembles

285   recent findings in the basolateral amygdala, where increased activity in some neurons were

286   correlated with the cessation of movement, irrespective of motivation or valence (Amir et al.,

287   2015, Pare and Quirk, 2017).

288   Previous work on PL has focused on its necessity for the expression of freezing during

289   fear conditioning (Baeg et al., 2001, Vidal-Gonzalez et al., 2006, Burgos-Robles et al., 2009,

290   Sierra-Mercado et al., 2011). However, in platform-mediated avoidance, freezing is either not

291   reduced (Bravo-Rivera et al., 2014) or is increased (present study) by pharmacological

292   inactivation of PL, suggesting that avoidance training alters the freezing circuit. Prior

293   manipulations of prefrontal, amygdala, and striatal areas dissociated the expression of

294   avoidance from the expression of freezing in this task (Bravo-Rivera et al., 2014, Rodriguez-

295   Romaguera et al., 2016). Furthermore, we observed that stimulation of PL at 4 Hz impaired

296   avoidance without increasing freezing. Thus, impaired avoidance is not a result of freezing-

297   induced blockade of avoidance (Lazaro-Munoz et al., 2010).

298   Neurons in rPL project to the ventral striatum (VS; Sesack et al., 1989, Vertes, 2004),

299   another region necessary for avoidance in this task (Bravo-Rivera et al., 2014) as well as other

300   avoidance tasks (Darvas et al., 2011, Ramirez et al., 2015, Hormigo et al., 2016). Inputs to VS

301   from rPL may be necessary for the initiation of platform-mediated avoidance via disinhibition of

302   VS output, similar to appetitive behaviors where inputs to VS must be inhibited to trigger

303   foraging for food (Rada et al., 1997, Saulskaya and Mikhailova, 2002, Do-Monte et al., 2017).

304   The VS also receives input from the basolateral amygdala (BLA; McDonald, 1991, Wright et al.,

305   1996, Groenewegen et al., 1999, Pitkänen et al., 2000), and this projection was recently

306   implicated in the expression of shuttle avoidance (Ramirez et al., 2015). One possibility is that

307   inputs from both rPL and BLA projecting to VS may be involved in avoidance, with rPL inputs

308   initiating early avoidance, and BLA inputs initiating late avoidance. Thus, as the tone progresses

309   and shock becomes more imminent, direct BLA inputs to VS are recruited. More work is needed

310   to test this hypothesis.

311   We delayed avoidance initiation by photostimulating at 4 Hz, which was the average

312   decrease in firing rate in neurons showing inhibitory responses to the tone. This rate of

313   stimulation is much lower than the 20+ Hz used in previous behavioral studies employing

314   channelrhodopsin (Liu et al., 2012, Felix-Ortiz and Tye, 2014, Marcinkiewcz et al., 2016,

315   Villaruel et al., 2017, Warlow et al., 2017). Moreover, we have previously observed that

316   photoactivation of infralimbic prefrontal cortex at rates ≥10 Hz was needed to reduce

317   conditioned freezing (Do-Monte et al., 2015a). As 4 Hz is close to the average firing rate of

318   mPFC putative projection neurons (Jung et al., 1998, Baeg et al., 2001, Burgos-Robles et al.,

319   2009, Sotres-Bayon et al., 2012), the delay in avoidance was likely due to a reduction of

320   neuronal inhibition rather than excitation above baseline. However, an important caveat is that

321   CamKIIα-expressing neurons were activated indiscriminately, and were not limited to neurons

322   showing inhibitory responses to the tone. Thus, in addition to reducing inhibitory responses in

323   one population of cells, we likely induced excitation in another population of cells that do not

324   normally express inhibitory tone responses. Both mechanisms would have the effect of

325   increasing tone-induced activity at rPL targets, which could account for the more robust effect of

326   photoactivation vs. muscimol inactivation on the initiation of avoidance.

327   There are multiple sources of input to rPL capable of driving inhibition during the tone.

328   PL receives input from the BLA, vHPC, and OFC (Bacon et al., 1996, Vertes, 2006, Hoover and

329   Vertes, 2007). BLA inputs to rPL are tone-responsive and robust, however, they appear to be

330   excitatory (Orozco-Cabal et al., 2006, Little and Carter, 2012, Little and Carter, 2013),

331   communicating auditory conditioned responses (Senn et al., 2014, Cheriyan et al., 2016,

332   Burgos-Robles et al., 2017). Indeed, inactivating BLA reduces the CS-responsiveness of PL

333   neurons (Laviolette et al., 2005, Sotres-Bayon et al., 2012). A more likely candidate for inhibitory

334   input is the ventral hippocampus (vHPC), as inactivation of this area increases conditioned tone

335   responses of PL neurons (Sotres-Bayon et al., 2012). Consistent with this, other studies have

336   demonstrated that vHPC targets interneurons in the prefrontal cortex (Gabbott et al., 2002,

337   Ishikawa and Nakamura, 2003, Tierney et al., 2004). Whereas vHPC activity is necessary to

338   acquire fear (Maren and Holt, 2004, Sierra-Mercado et al., 2011, Chen et al., 2016), it is

339   unknown whether vHPC activity is necessary for avoidance.

340   Excessive avoidance of stimuli that are not dangerous is clinically relevant for PTSD and

341   other anxiety disorders. Rodent PL is thought to be homologous to the dorsal anterior cingulate

342   (dACC) in humans (Bicks et al., 2015, Heilbronner et al., 2016). Although it is difficult to link unit

343   recording findings with BOLD responses in fMRI studies, decreased activity in human dACC

344   was correlated with active avoidance (Schlund et al., 2015), and avoidance has been correlated

345   with functional connectivity between rostral dACC and striatum (Collins et al., 2014). In PTSD

346   patients, avoidance symptoms correlate with excessive activity in rostral dACC (Marin et al.,

347   2016). Together with our findings, this suggests that compromised inhibitory control of rostral

348   dACC may predispose individuals to express avoidance when it competes with a high

349   behavioral cost, and/or when it is not urgent.

350 **Methods**

351 *Subjects*

352   A total of 156 adult male Sprague Dawley rats (Harlan Laboratories, Indianapolis, IN)

353 aged 3-5 months and weighing 320-420 g were housed and handled as previously described

354 (Bravo-Rivera et al., 2014). Rats were maintained on a restricted diet (18 g/day) of standard

355 laboratory rat chow to facilitate pressing a bar for food on a variable interval schedule of

356 reinforcement (VI-30). All procedures were approved by the Institutional Animal Care and Use

357 Committee of the University of Puerto Rico School of Medicine in compliance with the National

358 Institutes of Health guidelines for the care and use of laboratory animals.

359 *Surgery*

360   Rats were anesthetized with isofluorane inhalant gas (5%) first in an induction chamber

361 then positioned in a stereotaxic frame (Kopf Instruments, Tujunga, CA). Isofluorane (2-3%) was

362 delivered through a facemask for anesthesia maintenance. For pharmacological inactivations,

363 rats were implanted with 26-gauge double guide cannulas (Plastics One, Roanoke, VA) in the

364 prelimbic prefrontal cortex (PL; +3.0 mm AP; ±0.6 mm ML; -2.5 mm DV, 0º angle) to bregma).

365 For optogenetic experiments, rats were bilaterally implanted with 22-gauge single guide

366 cannulas (Plastics One, Roanoke, VA) in the prelimbic prefrontal cortex (PL; +2.6-2.8 mm AP;

367 ±1.50 mm ML; -3.40 mm DV to bregma, 15°angle). An injector extending 2 mm beyond the tip of

368 each cannula was used to infuse 0.5 μl of virus at a rate of 0.05 μl/min. The injector was kept

369 inside the cannula for an additional 10 min to reduce back-flow. The injector was then removed

370 and an optical fiber (0.22 NA, 200 nm core, constructed with products from Thorlabs, Newton,

371 NJ) with 1 mm of projection beyond the tip of each cannula was inserted for PL illumination. The

372 guide cannula and the optical fiber were cemented to the skull (C&B metabond, Parkell,

373 Brentwood, NY; Ortho Acrylic, Bayamón, PR). For unit recording experiments, rats were

374 implanted with a moveable array of 9 or 16 microwires (50 μm spacing, 3x3 or 2 x 8, Neuro

375 Biological Laboratories, Denison, TX) targeting regions of PL along the rostral-caudal axis. After

376   surgery, triple antibiotic was applied topically around the surgery incision, and an analgesic

377   (Meloxicam, 1 mg/Kg) was injected subcutaneously. Rats were allowed a minimum of 7 days to

378   recover from surgery prior to behavioral training.

379   *Behavior*

380   Rats were initially trained to press a bar to receive food pellets on a variable interval

381   reinforcement schedule (VI-30) inside standard operant chambers (Coulbourn Instruments,

382   Whitehall, PA) located in sound-attenuating cubicles (MED Associates, St. Albans, VT). Bar-

383   pressing was used to maintain a constant level of activity against which avoidance and freezing

384   could reliably be measured. Rats were trained until they reached a criterion of ≥15 presses/min.

385   Rats pressed for food throughout all phases of the experiment.

386   For platform-mediated avoidance, rats were trained as previously described (Bravo-

387   Rivera et al., 2014). Briefly, rats were conditioned with a pure tone (30 s, 4 kHz, 75 dB) co-

388   terminating with a scrambled shock delivered through the floor grids (2 s, 0.4 mA). The inter-trial

389   interval was variable, averaging 3 min. An acrylic square platform (14.0 cm each side, 0.33 cm

390   tall) located in the opposite corner of the sucrose pellet–delivering bar protected rats from the

391   shock. The platform was fixed to the floor and was present during all stages of training

392   (including bar-press training). Rats were conditioned for 10 days, with 9 tone-shock pairings per

393   day with a VI-30 schedule maintained across all training and test sessions. The availability of

394   food on the side opposite to the platform motivated rats to leave the platform during the inter-

395   trial interval, facilitating trial-by-trial assessment of avoidance. Once rats learned platform-

396   mediated avoidance, rats underwent a 2-tone expression test (2 tones with no shock).

397   *Drug infusions*

398   The GABA-A agonist muscimol (fluorescent muscimol, BODIPY TMR-X conjugate,

399   Sigma-Aldrich) was used to enhance GABA-A receptor activity, thereby inactivating target

400   structures. Infusions were made 45 min before testing at a rate of 0.2 µl/min (0.11 nmol/ 0.2 µl/

401   per side), similar to our previous studies (Do-Monte et al., 2015b, Rodriguez-Romaguera et al.,

402   2016).

403   *Viruses*

404   The adeno-associated viruses (AAVs; serotype 5) were obtained from the University of

405   North Carolina Vector Core (Chapel Hill, NC). Viral titers were 4 x 10^{12} particles/ml for

406   channelrhodopsin (AAV5:CaMKIIα::hChR2(H134R)-eYFP) and archaerhodopsin

407   (AAV5:CaMKIIα::eArchT3.0-eYFP) and 3 x 10^{12} particles/ml for control (AAV5:CaMKIIα::eYFP).

408   Rats expressing eYFP in PL were used to control for any nonspecific effects of viral infection or

409   laser heating. The CaMKIIα promoter was used to enable transgene expression favoring

410   pyramidal neurons (Liu and Jones, 1996). Viruses were housed in a -80º C freezer until the day

411   of infusion.

412   *Laser delivery*

413   Rats expressing channelrhodopsin (ChR2) in PL were illuminated using a blue diode-

414   pump solid state laser (DPSS, 473 nm, 2 or 4 Hz, 5 ms pulse width, 8-10 mW at the optical fiber

415   tip; OptoEngine, Midvale, UT), similar to our previous study (Do-Monte et al., 2015a). Rats

416   expressing archaerhodopsin (Arch) in PL were bilaterally illuminated using a DPSS green laser

417   (532 nm, constant, 10-12 mW at the optical fiber tip; OptoEngine). For both ChR2 and Arch

418   experiments, the laser was activated at tone onset and persisted throughout the 30 s tone

419   presentation. Laser light was passed through a shutter/coupler (200 nm, Oz Optics, Ontario,

420   Canada), patchcord (200 nm core, ThorLabs, Newton, NJ), rotary joint (200 nm core, 2 x 2,

421   Doric Lenses, Quebec city, Canada), dual patchcord (0.22 NA, 200 nm core, ThorLabs), and

422   bilateral optical fibers (made in-house with materials from ThorLabs and Precision Fiber

423   Products, Milpitas, CA) targeting the specific subregions in PL. Rats were familiarized with the

424   patchcord during bar press training and during the last 4 d of avoidance training before the

425   expression test.

426   *Single-unit recordings*

427   Rats implanted with moveable electrode arrays targeting PL were either avoidance

428   conditioned as previously described or exposed to the training environment (platform, tone

429   presentations, behavior box) in the absence of the shock. Extracellular waveforms that

430   exceeded a voltage threshold were digitized at 40 kHz and stored on a computer. Waveforms

431   were then sorted offline using three-dimensional plots of principal component and voltage

432   vectors (Offline Sorter; Plexon, Dallas, TX) and clusters formed by individual neurons were

433   tracked. Timestamps of neural spiking and flags for the occurrence of tones and shocks were

434   imported to NeuroExplorer for analysis (NEX Technologies, Madison, AL). Because we used a

435   high impedance electrode in the current study (~750-1000 kOhm), we were unable to sample

436   interneurons. Data was recorded during the entire session except during the 2 sec shock. After

437   conditioning, rats were tested for avoidance expression. For avoidance assessment, rats

438   received full conditioning sessions (with shocks) across days. Inclusion of the shock prevented

439   extinction of avoidance. After each day, electrodes were lowered 150 µM to isolate new neurons

440   for the following session the next day. To detect tone-elicited changes in PL activity, we

441   assessed whether neurons changed their firing rate significantly during the first 500-1000 ms

442   after tone onset across the first 5 trials. A Z-score for each 500 ms bin was calculated relative to

443   20 pre-tone bins of equal duration (10 sec pre-tone). PL neurons were classified as showing

444   excitatory tone responses if the initial bins exceeded 2.58 z's ($p < 0.01$, two-tailed). PL neurons

445   were classified as showing inhibitory tone responses across time if any of the initial two tone

446   bins exceeded -1.96 Z's ($p < 0.05$, two-tailed). To detect changes in PL activity during platform

447   entry, we employed the same procedure used for assessing tone responses. We assessed

448   whether neurons changed their firing rate significantly during the first 500-1000 ms after

449   platform entry. A Z-score for each 500 ms bin was calculated relative to the same pre-tone

450   baseline. Heat maps of single unit data were generated with Z-scores from baseline through the

451   28 sec after tone onset or platform entry.

452   *Optrode recordings*

453   Rats expressing Arch or ChR2 in PL were anesthetized with urethane (1g/Kg, i.p.; Sigma

454   Aldrich) and mounted in a stereotaxic frame. An optrode consisting of an optical fiber

455   surrounded by 8 or 16 single-unit recording wires (Neuro Biological Laboratories) was inserted

456   and aimed at PL (AP, +2.8 mm; ML: -0.5; DV: -3.5). The optrode was ventrally advanced in

457   steps of 0.03 mm. Single-units were monitored in real time (RASPUTIN, Plexon). After isolating

458   a single-unit, a 532 nm laser was activated for 10 sec within a 20 sec period, at least 10 times

459   for Arch-infected PL neurons. For ChR2-infected PL neurons, a 473 nm laser was activated for

460   30s at a rate of 2 or 4 Hz (5 ms pulse width) within a 90s period (60s ITI), at least 5 times.

461   Single-units were recorded and stored for spike sorting (Offline Sorter, Plexon) and spike-train

462   analysis (Neuorexplorer, NEX Technologies). Excitatory and inhibitory responses were

463   calculated by comparing the average firing rate of each neuron during the 10 sec of laser OFF

464   with the 10 sec of laser ON for Arch neurons and during 30 sec laser OFF just prior to the 30

465   sec of laser ON for ChR2 neurons (Paired t-test, 1 s bins).

466   *Open field task*

467   Locomotor activity in the open field arena (90 cm diameter) was automatically assessed

468   (ANY-Maze) by comparing the total distance travelled between 30 sec trials (laser off versus

469   laser on), following a 3 min acclimation period for optogenetic experiments. The distance

470   traveled was used to assess locomotion and time in center was used to assess anxiety. For

471   pharmacological inactivation experiments, distance traveled and time in center was measured

472   over a 3 min period following a 3 min acclimation period 45 min after MUS or SAL was infused

473   prior to sacrificing animals.

474   *Histology*

475   After behavioral experiments, rats were deeply anesthetized with sodium pentobarbital

476   (450 mg/kg i.p.) and transcardially perfused with 0.9 % saline followed by a 10 % formalin

477   solution. Brains were removed from the skull and stored in 30 % sucrose for cryoprotection for

478   at least 72 h before sectioning and Nissl staining. Histology was analyzed for placement of

479   cannulas, virus expression, and electrodes.

480   *Data Collection and Analysis*

481   Behavior was recorded with digital video cameras (Micro Video Products, Peterborough,

482   Ontario, Canada). Freezing and platform avoidance was quantified by observers blind to the

483   experimental group. Freezing was defined as the absence of all movement except for

484   respiration. Avoidance was defined as the rat having at least three paws on the platform. In a

485   subset of animals, AnyMaze software was available for recording and calculating freezing and

486   avoidance (Stoelting, Wood Dale, IL). The time spent avoiding during the tone (percent time on

487   platform) was used as our avoidance measure. Avoidance and freezing to the tone was

488   expressed as a percentage of the 30 second tone presentation. Our experimental groups

489   typically consisted of approximately 15 animals. This is typical of other laboratories and results

490   in sufficient statistical confidence. Moreover, it also agrees with the theoretical minimum sample

491   size given by:

492    $$n = \frac{z^2 \sigma^2}{d^2}$$

493   where z = the level of confidence desired (in standard deviations), σ = the estimate of the

494   population standard deviation, and d = the acceptable width of the confidence interval.

495   Technical replications, testing the same measurement multiple times, and biological

496   replications, performing the same test on multiple samples (individual rats or single units), were

497   used to test the variability in each experiment. Statistical significance was determined with

498   Student's two-tailed t-tests, Fisher Exact tests, Chi Square tests, Mann Whitney U tests, or

499   repeated-measures ANOVA, followed by post hoc Tukey analysis, and Bonferroni corrections,

500   where appropriate using STATISTICA (Statsoft, Tulsa, OK) and Prism (Graphpad, La Jolla, CA).

501

502   Figure Legends.

503   **Figure 1**. **Pharmacological inactivation of prelimbic cortex delays avoidance. A.**

504   Schematic of MUS infusion showing min (dark orange) and max (light orange) extent of infusion

505   in PL. **B.** Rats were trained across 10 days to avoid a tone-signaled foot-shock by stepping onto

506   a platform. On Day 11, rats received 2 tone presentations (without shock) 45 min after MUS

507   infusion. On Day 12, rats received a second 2-tone test drug free. **C.** Percent time on platform

508   during Tone 1 on Days 10, 11 (with MUS), and 12 for saline controls (SAL, n=17; grey) and

509   MUS rats (n=13, orange). **D.** Time spent on platform in 3 sec bins (Tone 1, Test 1) revealed that

510   MUS rats were significantly delayed in their avoidance compared to SAL controls (repeated

511   measures ANOVA, post hoc Tukey test). **E.** Latency of avoidance for each rat (Mann Whitney U

512   Test, Tone 1, Test 1). *Inset*: Effect of MUS inactivation (Tone 1, test 1) on freezing during the

513   tone (unpaired t-test). Data are shown as mean ± SEM; *p<0.05, **p<0.01.

514

515   **Figure 2. Optogenetic silencing of prelimbic neurons does not delay avoidance. A.** *Left*:

516   Schematic of Arch expression and optrode placement (n=2 rats). *Middle*: Rasters and

517   peristimulus time histogram of a single PL neuron showing a decrease in firing rate during laser

518   illumination (8-10mW, 532nm, 10s ON, 10s OFF, 10 trials). *Right*: Proportion of PL neurons that

519   exhibited a decrease (blue, n=41), increase (gold, n=11), or no change (grey, n=18) in firing

520   rate. **B**. Schematic of virus infusion, location of min/max expression of AAV in rPL (pink) and

521   cPL (purple), followed by avoidance training and test. At Test, 532nm light was delivered to rPL

522   or cPL during the entire 30-second tone presentation (Tone 1). **C**. *Left*: Micrograph of Arch

523   expression and optical fiber placement in rPL. *Right*: Percent time on platform at Cond (Day 10,

524   Tone 1) and Test (Day 11, Tone 1 with laser ON and Tone 2 with laser OFF) for eYFP-rPL

525   control (n=15, grey) and Arch-rPL rats (n=17, green). **D**. *Left*: Micrograph of Arch expression

526   and optical fiber placement in cPL. *Right*: Percent time on platform during Cond and Test for

527   eYFP-cPL control (n=7, grey) and Arch-cPL rats (n=9, green). **E**. *Left*: Time spent on platform in

528   3 sec bins (Tone 1 at Test) revealed no effect of silencing rPL-Arch neurons compared to eYFP

529   controls (repeated measures ANOVA, post hoc Tukey test). *Right*: Latency of avoidance for

530   each rat (Tone 1 at Test). rPL-Arch rats showed a decrease in avoidance latency (Mann

531   Whitney U test, p<0.05). **F**. Timeline of avoidance (left) and latency (right) for cPL-eYFP control

532   rats and cPL-Arch rats. All data are shown as mean ± SEM; p<0.05.

533

534   **Figure 3. Initiation of avoidance is correlated with inhibition in rostral PL neurons. A**.

535   Location of recordings across PL (n=7 avoidance-trained and n=8 naïve rats). **B**. *Left*: Cartoon

536   of rat behavior at tone onset during unit recordings. *Right*: single unit examples of an excitatory

537   (gold rasters) and inhibitory tone response (blue rasters). Each row represents a single trial. **C**.

538   Percentage of neurons that were excitatory (gold) or inhibitory (blue) throughout the tone. Time

539   of platform entry (black dots), for all successful trials (n=340) in avoidance rats is indicated

540   relative to tone onset. **D**. *Left*: Heat map of normalized responses (z-score) to tone onset (Time

541   = 0 sec) of neurons in avoidance rats. Each row represents one neuron, bin = 0.5 sec. Arrows

542   indicate bins used to determine criteria for excitatory (gold, first 500ms bin), or inhibitory (blue,

543   first or second 500ms bin) tone responses. *Right:* Pie charts showing proportions of neurons

544   that were excited, inhibited, or non-responsive at tone onset in avoidance (n = 34, 25, 182,

545   respectively), naïve (n = 20, 3, 143, respectively), and fear conditioned rats (n = 25, 3, 163,

546   respectively). Proportion of inhibitory responses were significantly greater in avoidance rats

547   compared to naïve and fear rats (Chi Square test, **p<0.001). *Bottom*: Percentage of cells that

548   were excited in avoidance (gold) or naïve (light gold) rats (left) or inhibited in avoidance (blue) or

549   naïve (light blue) rats (right) around tone onset (Fisher exact tests). **E**. *Left*: Cartoon of rat

550   entering platform after tone onset during unit recordings. *Right*: single unit examples of an

551   excitatory (gold rasters) and inhibitory platform entry response (blue rasters). **F**. Percentage of

552   neurons that were excitatory (gold) or inhibitory (blue) at platform entry. Time of tone onset

553   (black dots), for all successful trials (n=340) in avoidance rats is indicated relative to platform

554   entry. **G**. *Left*: Heat map of normalized responses to platform entry (Time = 0 sec) of neurons in

555   avoidance rats. *Right*: Pie charts showing proportions of neurons that were excited, inhibited, or

556   non-responsive at platform entry in avoidance (n = 40, 22, 156, respectively) and naïve rats (n =

557   23, 10, 127, respectively). *Bottom*: Percentage of cells that were excited in avoidance (gold) or

558   naïve (light gold) rats (left) or inhibited in avoidance (blue) or naïve (light blue) rats (right) after

559   platform entry (Fisher exact tests). **H**. Tone responsive neurons were not responsive to platform

560   entry. All data are shown as mean ± SEM; *p<0.05, **p<0.01.

561

562   **Figure 4. Characterization of inhibitory tone responsive neurons. A**. Normalized firing rate

563   of cells that were inhibited for less than 15 sec (dark blue) or more than 15 sec (light blue) after

564   tone onset. **B**. Average inhibitory response of neurons decreased from a baseline firing rate of

565   5.8 Hz to 1.98 Hz at tone onset. **C**. *Left*: sagittal view of location of inhibitory tone responsive

566   neurons in rPL (blue) or cPL (purple). *Right*: Histological analysis revealed that more inhibited

567   neurons were located in rPL (Fisher Exact Test). **D**. Classification of PL neurons into putative

568   projection neurons (gray triangle) or interneurons (gray circle) based on spike width and

569   baseline firing rate (Sotres-Bayon et al, 2012). Neurons showing inhibitory responses

570   (blue/purple, n=25) were likely projection neurons. All data are shown as mean ± SEM; *p<0.05.

571

572   **Figure 5. 4 Hz photoactivation and single unit recordings of rostral PL neurons in**

573   **anesthetized rats. A**. Schematic of ChR2 expression and optrode placement (n=4 rats). **B**.

574   Rasters and peristimulus time histograms of a representative single neuron showing increased

575   firing rate during laser illumination (8-10mW, 473nm, 30s ON, 30s OFF, 4 Hz, 5 trials). **C**. *Left*:

576   Proportion of neurons showing an increase (gold, n=43), decrease (blue, n=27), or no change

577   (grey, n=42) in firing rate with laser ON. *Right*: Average firing rate at baseline (dark grey) and 4

578   Hz photoactivation for neurons showing increased (gold) changes in firing rate. **D**. Rasters and

579   peristimulus time histograms of a representative single neuron showing increased firing rate

580   during laser illumination (8-10mW, 473nm, 30s ON, 30s OFF, 2 Hz, 5 trials). **E**. *Left*: Proportion

581   of neurons showing an increase (n=35), decrease (n=26), or no change (n=15) in firing rate with

582   laser ON. *Right*: Average firing rate at baseline, and 2 Hz photoactivation for neurons showing

583   increased changes in firing rate. All data are shown as mean ± SEM.

584

585   **Figure 6. 4 Hz photoactivation of rostral PL neurons during the tone delays or prevents**

586   **avoidance. A**. Schematic of viral infusion and location of min/max spread of AAV expression in

587   rPL (pink) and cPL (purple), followed by avoidance training and test. At Test, 473nm light was

588   delivered to rPL or cPL during the first 30-second tone presentation (Tone 1). **B**. *Left*:

589   Micrograph of ChR2 expression and optical fiber placement in rPL. *Right*: Percent time on

590   platform at Cond (Day 10, Tone 1) and Test (Day 11, Tone 1 with laser ON and Tone 2 with

591   laser OFF) for eYFP-rPL control rats (grey, n=9) and ChR2-rPL rats (blue, n=14). **C**. *Left*:

592   Micrograph of ChR2 expression and optical fiber placement in cPL. *Right*: Percent time on

593   platform during Cond and Test for eYFP-cPL control rats (grey, n=7) and ChR2-cPL rats (blue,

594   n=9). **D**. *Left*: Time spent on platform in 3 sec bins (Tone 1 at Test) revealed that rPL-ChR2 rats

595   were significantly delayed in their avoidance compared to eYFP controls (repeated measures

596   ANOVA, post hoc Tukey test). *Right*: Latency of avoidance for each rat (Mann Whitney U Test,

597   Tone 1 at Test). 7/14 rats never avoided. *Inset*: 4 Hz photoactivation in rPL had no effect on

598   freezing (Tone 1 at Test). **E**. Timeline of avoidance (left) and latency (right) for eYFP-cPL

599   control ChR2-cPL rats revealed no effect of 4 Hz photoactivation of caudal PL. **F**. Timeline of

600   avoidance (left) and latency (right) for eYFP-rPL control rats (grey, n=9) and ChR2-rPL rats

601   (blue, n=9) revealed no effect of 2 Hz photoactivation. **G**. Timeline of avoidance (left) and

602   latency (right) for eYFP-rPL control rats (grey, n=8) and ChR2-rPL rats (blue, n=13) revealed no

603   effect of 4Hz photoactivation during a 30 sec ITI period. **H**. Timeline of avoidance (left) and

604   latency (right) for eYFP-rPL control rats (grey, n=10) and ChR2-rPL rats (blue, n=9) revealed a

605   delay in the initiation of avoidance with 4Hz photoactivation during the first 15 sec of the tone

606   (Mann Whitney U test for time course and avoidance latency). All data are shown as mean ±

607   SEM; *p<0.05; **p<0.01.

608

609   **Video 1. 4 Hz photoactivation of rostral PL neurons during the tone impairs avoidance.**

610   Video of an individual rat with ChR2 infused into rPL showing avoidance behavior on the last

611   day of avoidance training (Day 10) at Tone 1, followed by the rat's behavior at Test (Day 11)

612   with the laser on during the tone (4 Hz, 30 sec duration, 5 ms pulse width, 8-10mW light

613   intensity).

614

615   References.

616   Amir, A., Lee, S. C., Headley, D. B., Herzallah, M. M. and Pare, D. (2015) 'Amygdala Signaling
617   during Foraging in a Hazardous Environment', *J Neurosci,* 35(38), pp. 12994-3005.
618   Bacon, S. J., Headlam, A. J., Gabbott, P. L. and Smith, A. D. (1996) 'Amygdala input to medial
619   prefrontal cortex (mPFC) in the rat: a light and electron microscope study', *Brain Res.,*
620   720(1-2), pp. 211-219.
621   Baeg, E. H., Kim, Y. B., Jang, J., Kim, H. T., Mook-Jung, I. and Jung, M. W. (2001) 'Fast spiking
622   and regular spiking neural correlates of fear conditioning in the medial prefrontal cortex
623   of the rat', *Cereb.Cortex,* 11(5), pp. 441-451.
624   Beck, K. D., Jiao, X., Smith, I. M., Myers, C. E., Pang, K. C. and Servatius, R. J. (2014) 'ITI-
625   Signals and Prelimbic Cortex Facilitate Avoidance Acquisition and Reduce Avoidance
626   Latencies, Respectively, in Male WKY Rats', *Front Behav Neurosci,* 8, pp. 403.
627   Bicks, L. K., Koike, H., Akbarian, S. and Morishita, H. (2015) 'Prefrontal Cortex and Social
628   Cognition in Mouse and Man', *Front Psychol,* 6, pp. 1805.
629   Bravo-Rivera, C., Roman-Ortiz, C., Brignoni-Perez, E., Sotres-Bayon, F. and Quirk, G. J. (2014)
630   'Neural structures mediating expression and extinction of platform-mediated avoidance',
631   *J Neurosci,* 34(29), pp. 9736-42.
632   Bravo-Rivera, C., Roman-Ortiz, C., Montesinos-Cartagena, M. and Quirk, G. J. (2015)
633   'Persistent active avoidance correlates with activity in prelimbic cortex and ventral
634   striatum', *Front Behav Neurosci,* 9, pp. 184.
635   Burgos-Robles, A., Bravo-Rivera, H. and Quirk, G. J. (2013) 'Prelimbic and infralimbic neurons
636   signal distinct aspects of appetitive instrumental behavior', *PLoS One,* 8(2), pp. e57575.
637   Burgos-Robles, A., Kimchi, E. Y., Izadmehr, E. M., Porzenheim, M. J., Ramos-Guasp, W. A.,
638   Nieh, E. H., Felix-Ortiz, A. C., Namburi, P., Leppla, C. A., Presbrey, K. N.,
639   Anandalingam, K. K., Pagan-Rivera, P. A., Anahtar, M., Beyeler, A. and Tye, K. M.
640   (2017) 'Amygdala inputs to prefrontal cortex guide behavior amid conflicting cues of
641   reward and punishment', *Nat Neurosci,* 20(6), pp. 824-835.
642   Burgos-Robles, A., Vidal-Gonzalez, I. and Quirk, G. J. (2009) 'Sustained conditioned responses
643   in prelimbic prefrontal neurons are correlated with fear expression and extinction failure',
644   *The Journal of neuroscience : the official journal of the Society for Neuroscience,* 29(26),
645   pp. 8474-82.
646   Chang, C. H., Berke, J. D. and Maren, S. (2010) 'Single-unit activity in the medial prefrontal
647   cortex during immediate and delayed extinction of fear in rats', *PLoS.One.,* 5(8), pp.
648   e11971.
649   Chen, V. M., Foilb, A. R. and Christianson, J. P. (2016) 'Inactivation of ventral hippocampus
650   interfered with cued-fear acquisition but did not influence later recall or discrimination',
651   *Behav Brain Res,* 296, pp. 249-253.
652   Cheriyan, J., Kaushik, M. K., Ferreira, A. N. and Sheets, P. L. (2016) 'Specific Targeting of the
653   Basolateral Amygdala to Projectionally Defined Pyramidal Neurons in Prelimbic and
654   Infralimbic Cortex', *eNeuro,* 3(2).
655   Chow, B. Y., Han, X., Dobry, A. S., Qian, X., Chuong, A. S., Li, M., Henninger, M. A., Belfort, G.
656   M., Lin, Y., Monahan, P. E. and Boyden, E. S. (2010) 'High-performance genetically
657   targetable optical neural silencing by light-driven proton pumps', *Nature,* 463(7277), pp.
658   98-102.
659   Ciocchi, S., Herry, C., Grenier, F., Wolff, S. B., Letzkus, J. J., Vlachos, I., Ehrlich, I., Sprengel,
660   R., Deisseroth, K., Stadler, M. B., Muller, C. and Luthi, A. (2010) 'Encoding of
661   conditioned fear in central amygdala inhibitory circuits', *Nature,* 468(7321), pp. 277-282.
662   Collins, K. A., Mendelsohn, A., Cain, C. K. and Schiller, D. (2014) 'Taking action in the face of
663   threat: neural synchronization predicts adaptive coping', *J Neurosci,* 34(44), pp. 14733-8.

664   Courtin, J., Chaudun, F., Rozeske, R. R., Karalis, N., Gonzalez-Campo, C., Wurtz, H., Abdi, A.,
665   Baufreton, J., Bienvenu, T. C. and Herry, C. (2014) 'Prefrontal parvalbumin interneurons
666   shape neuronal activity to drive fear expression', *Nature,* 505(7481), pp. 92-6.
667   Darvas, M., Fadok, J. P. and Palmiter, R. D. (2011) 'Requirement of dopamine signaling in the
668   amygdala and striatum for learning and maintenance of a conditioned avoidance
669   response', *Learning & memory,* 18(3), pp. 136-43.
670   Do Monte, F. H., Quirk, G. J., Li, B. and Penzo, M. A. (2016) 'Retrieving fear memories, as time
671   goes by…', *Mol Psychiatry,* 21(8), pp. 1027-36.
672   Do-Monte, F. H., Manzano-Nieves, G., Quiñones-Laracuente, K., Ramos-Medina, L. and Quirk,
673   G. J. (2015a) 'Revisiting the role of infralimbic cortex in fear extinction with optogenetics',
674   *J Neurosci,* 35(8), pp. 3607-15.
675   Do-Monte, F. H., Minier-Toribio, A., Quiñones-Laracuente, K., Medina-Colón, E. M. and Quirk,
676   G. J. (2017) 'Thalamic Regulation of Sucrose Seeking during Unexpected Reward
677   Omission', *Neuron,* 94(2), pp. 388-400.e4.
678   Do-Monte, F. H., Quiñones-Laracuente, K. and Quirk, G. J. (2015b) 'A temporal shift in the
679   circuits mediating retrieval of fear memory', *Nature,* 519(7544), pp. 460-3.
680   DSM–V (ed.) (2013) *Diagnostic and statistical manual of mental disorders (5th ed., text rev.).*
681   Ehrlich, I., Humeau, Y., Grenier, F., Ciocchi, S., Herry, C. and Luthi, A. (2009) 'Amygdala
682   inhibitory circuits and the control of fear memory', *Neuron.,* 62(6), pp. 757-771.
683   Felix-Ortiz, A. C. and Tye, K. M. (2014) 'Amygdala inputs to the ventral hippocampus
684   bidirectionally modulate social behavior', *J Neurosci,* 34(2), pp. 586-95.
685   Floyd, N. S., Price, J. L., Ferry, A. T., Keay, K. A. and Bandler, R. (2000) 'Orbitomedial
686   prefrontal cortical projections to distinct longitudinal columns of the periaqueductal gray
687   in the rat', *J.Comp Neurol.,* 422(4), pp. 556-578.
688   Floyd, N. S., Price, J. L., Ferry, A. T., Keay, K. A. and Bandler, R. (2001) 'Orbitomedial
689   prefrontal cortical projections to hypothalamus in the rat', *J.Comp Neurol.,* 432(3), pp.
690   307-328.
691   Gabbott, P., Headlam, A. and Busby, S. (2002) 'Morphological evidence that CA1 hippocampal
692   afferents monosynaptically innervate PV-containing neurons and NADPH-diaphorase
693   reactive cells in the medial prefrontal cortex (Areas 25/32) of the rat', *Brain Res,* 946(2),
694   pp. 314-22.
695   Giustino, T. F. and Maren, S. (2015) 'The Role of the Medial Prefrontal Cortex in the
696   Conditioning and Extinction of Fear', *Front Behav Neurosci,* 9, pp. 298.
697   Groenewegen, H. J., Wright, C. I., Beijer, A. V. and Voorn, P. (1999) 'Convergence and
698   segregation of ventral striatal inputs and outputs', *Ann N Y Acad Sci,* 877, pp. 49-63.
699   Han, X., Chow, B. Y., Zhou, H., Klapoetke, N. C., Chuong, A., Rajimehr, R., Yang, A., Baratta,
700   M. V., Winkle, J., Desimone, R. and Boyden, E. S. (2011) 'A high-light sensitivity optical
701   neural silencer: development and application to optogenetic control of non-human
702   primate cortex', *Frontiers in systems neuroscience,* 5, pp. 18.
703   Heilbronner, S. R., Rodriguez-Romaguera, J., Quirk, G. J., Groenewegen, H. J. and Haber, S.
704   N. (2016) 'Circuit-Based Corticostriatal Homologies Between Rat and Primate', *Biol
705   Psychiatry,* 80(7), pp. 509-21.
706   Herry, C. and Johansen, J. P. (2014) 'Encoding of fear learning and memory in distributed
707   neuronal circuits', *Nat Neurosci,* 17(12), pp. 1644-54.
708   Hoover, W. B. and Vertes, R. P. (2007) 'Anatomical analysis of afferent projections to the medial
709   prefrontal cortex in the rat', *Brain Struct.Funct.,* 212(2), pp. 149-179.
710   Hormigo, S., Vega-Flores, G. and Castro-Alamancos, M. A. (2016) 'Basal Ganglia Output
711   Controls Active Avoidance Behavior', *J Neurosci,* 36(40), pp. 10274-10284.
712   Hosking, J. G., Cocker, P. J. and Winstanley, C. A. (2016) 'Prefrontal Cortical Inactivations
713   Decrease Willingness to Expend Cognitive Effort on a Rodent Cost/Benefit Decision-
714   Making Task', *Cereb Cortex,* 26(4), pp. 1529-38.

715 Ishikawa, A. and Nakamura, S. (2003) 'Convergence and interaction of hippocampal and
716   amygdalar projections within the prefrontal cortex in the rat', *J.Neurosci.,* 23(31), pp.
717   9987-9995.
718 Isogawa, K., Bush, D. E. and LeDoux, J. E. (2013) 'Contrasting effects of pretraining,
719   posttraining, and pretesting infusions of corticotropin-releasing factor into the lateral
720   amygdala: attenuation of fear memory formation but facilitation of its expression',
721   *Biological psychiatry,* 73(4), pp. 353-9.
722 Jiao, X., Beck, K. D., Myers, C. E., Servatius, R. J. and Pang, K. C. (2015) 'Altered activity of the
723   medial prefrontal cortex and amygdala during acquisition and extinction of an active
724   avoidance task', *Front Behav Neurosci,* 9, pp. 249.
725 Johansen, J. P., Cain, C. K., Ostroff, L. E. and LeDoux, J. E. (2011) 'Molecular mechanisms of
726   fear learning and memory', *Cell,* 147(3), pp. 509-24.
727 Jung, M. W., Qin, Y., McNaughton, B. L. and Barnes, C. A. (1998) 'Firing characteristics of deep
728   layer neurons in prefrontal cortex in rats performing spatial working memory tasks',
729   *Cereb Cortex,* 8(5), pp. 437-50.
730 Laviolette, S. R., Lipski, W. J. and Grace, A. A. (2005) 'A subpopulation of neurons in the medial
731   prefrontal cortex encodes emotional learning with burst and frequency codes through a
732   dopamine D4 receptor-dependent basolateral amygdala input', *J.Neurosci.,* 25(26), pp.
733   6066-6075.
734 Lazaro-Munoz, G., LeDoux, J. E. and Cain, C. K. (2010) 'Sidman instrumental avoidance initially
735   depends on lateral and basal amygdala and is constrained by central amygdala-
736   mediated Pavlovian processes', *Biological psychiatry,* 67(12), pp. 1120-7.
737 LeDoux, J. E., Moscarello, J., Sears, R. and Campese, V. (2017) 'The birth, death and
738   resurrection of avoidance: a reconceptualization of a troubled paradigm', *Mol Psychiatry,*
739   22(1), pp. 24-36.
740 Little, J. P. and Carter, A. G. (2012) 'Subcellular synaptic connectivity of layer 2 pyramidal
741   neurons in the medial prefrontal cortex', *J Neurosci,* 32(37), pp. 12808-19.
742 Little, J. P. and Carter, A. G. (2013) 'Synaptic mechanisms underlying strong reciprocal
743   connectivity between the medial prefrontal cortex and basolateral amygdala', *J Neurosci,*
744   33(39), pp. 15333-42.
745 Liu, X., Ramirez, S., Pang, P. T., Puryear, C. B., Govindarajan, A., Deisseroth, K. and
746   Tonegawa, S. (2012) 'Optogenetic stimulation of a hippocampal engram activates fear
747   memory recall', *Nature,* 484(7394), pp. 381-5.
748 Liu, X. B. and Jones, E. G. (1996) 'Localization of alpha type II calcium calmodulin-dependent
749   protein kinase at glutamatergic but not gamma-aminobutyric acid (GABAergic) synapses
750   in thalamus and cerebral cortex', *Proc Natl Acad Sci U S A,* 93(14), pp. 7332-6.
751 Marcinkiewcz, C. A., Mazzone, C. M., D'Agostino, G., Halladay, L. R., Hardaway, J. A., DiBerto,
752   J. F., Navarro, M., Burnham, N., Cristiano, C., Dorrier, C. E., Tipton, G. J.,
753   Ramakrishnan, C., Kozicz, T., Deisseroth, K., Thiele, T. E., McElligott, Z. A., Holmes, A.,
754   Heisler, L. K. and Kash, T. L. (2016) 'Serotonin engages an anxiety and fear-promoting
755   circuit in the extended amygdala', *Nature,* 537(7618), pp. 97-101.
756 Maren, S. and Holt, W. G. (2004) 'Hippocampus and Pavlovian fear conditioning in rats:
757   muscimol infusions into the ventral, but not dorsal, hippocampus impair the acquisition of
758   conditional freezing to an auditory conditional stimulus', *Behav.Neurosci.,* 118(1), pp. 97-
759   110.
760 Marin, M. F., Song, H., VanElzakker, M. B., Staples-Bradley, L. K., Linnman, C., Pace-Schott, E.
761   F., Lasko, N. B., Shin, L. M. and Milad, M. R. (2016) 'Association of Resting Metabolism
762   in the Fear Neural Network With Extinction Recall Activations and Clinical Measures in
763   Trauma-Exposed Individuals', *Am J Psychiatry,* 173(9), pp. 930-8.
764 Martinez, R. C., Gupta, N., Lazaro-Munoz, G., Sears, R. M., Kim, S., Moscarello, J. M., LeDoux,
765   J. E. and Cain, C. K. (2013) 'Active vs. reactive threat responding is associated with

differential c-Fos expression in specific regions of amygdala and prefrontal cortex', *Learning & memory,* 20(8), pp. 446-52.

McDonald, A. J. (1991) 'Topographical organization of amygdaloid projections to the caudatoputamen, nucleus accumbens, and related striatal-like areas of the rat brain', *Neuroscience,* 44(1), pp. 15-33.

Moscarello, J. M. and LeDoux, J. E. (2013) 'Active avoidance learning requires prefrontal suppression of amygdala-mediated defensive reactions', *J Neurosci,* 33(9), pp. 3815-23.

Orozco-Cabal, L., Pollandt, S., Liu, J., Vergara, L., Shinnick-Gallagher, P. and Gallagher, J. P. (2006) 'A novel rat medial prefrontal cortical slice preparation to investigate synaptic transmission from amygdala to layer V prelimbic pyramidal neurons', *J Neurosci Methods,* 151(2), pp. 148-58.

Pare, D. and Quirk, G. J. (2017) 'When scientific paradigms lead to tunnel vision: lessons from the study of fear', 2, pp. 6.

Pendyam, S., Bravo-Rivera, C., Burgos-Robles, A., Sotres-Bayon, F., Quirk, G. J. and Nair, S. S. (2013) 'Fear signaling in the prelimbic-amygdala circuit: a computational modeling and recording study', *Journal of neurophysiology,* 110(4), pp. 844-61.

Pitkänen, A., Jolkkonen, E. and Kemppainen, S. (2000) 'Anatomic heterogeneity of the rat amygdaloid complex', *Folia Morphol (Warsz),* 59(1), pp. 1-23.

Rada, P., Tucci, S., Murzi, E. and Hernández, L. (1997) 'Extracellular glutamate increases in the lateral hypothalamus and decreases in the nucleus accumbens during feeding', *Brain Res,* 768(1-2), pp. 338-40.

Ramirez, F., Moscarello, J. M., LeDoux, J. E. and Sears, R. M. (2015) 'Active avoidance requires a serial basal amygdala to nucleus accumbens shell circuit', *J Neurosci,* 35(8), pp. 3470-7.

Rodriguez-Romaguera, J., Greenberg, B. D., Rasmussen, S. A. and Quirk, G. J. (2016) 'An Avoidance-Based Rodent Model of Exposure With Response Prevention Therapy for Obsessive-Compulsive Disorder', *Biol Psychiatry,* 80(7), pp. 534-40.

Saulskaya, N. B. and Mikhailova, M. O. (2002) 'Feeding-induced decrease in extracellular glutamate level in the rat nucleus accumbens: dependence on glutamate uptake', *Neuroscience,* 112(4), pp. 791-801.

Schlund, M. W., Brewer, A. T., Richman, D. M., Magee, S. K. and Dymond, S. (2015) 'Not so bad: avoidance and aversive discounting modulate threat appraisal in anterior cingulate and medial prefrontal cortex', *Front Behav Neurosci,* 9, pp. 142.

Senn, V., Wolff, S. B., Herry, C., Grenier, F., Ehrlich, I., Gründemann, J., Fadok, J. P., Müller, C., Letzkus, J. J. and Lüthi, A. (2014) 'Long-range connectivity defines behavioral specificity of amygdala neurons', *Neuron,* 81(2), pp. 428-37.

Sesack, S. R., Deutch, A. Y., Roth, R. H. and Bunney, B. S. (1989) 'Topographical organization of the efferent projections of the medial prefrontal cortex in the rat: an anterograde tract-tracing study with Phaseolus vulgaris leucoagglutinin', *J Comp Neurol,* 290(2), pp. 213-42.

Sierra-Mercado, D., Padilla-Coreano, N. and Quirk, G. J. (2011) 'Dissociable roles of prelimbic and infralimbic cortices, ventral hippocampus, and basolateral amygdala in the expression and extinction of conditioned fear', *Neuropsychopharmacology,* 36(2), pp. 529-538.

Sotres-Bayon, F., Sierra-Mercado, D., Pardilla-Delgado, E. and Quirk, G. J. (2012) 'Gating of fear in prelimbic cortex by hippocampal and amygdala inputs', *Neuron,* 76(4), pp. 804-12.

Sparta, D. R., Hovelsø, N., Mason, A. O., Kantak, P. A., Ung, R. L., Decot, H. K. and Stuber, G. D. (2014) 'Activation of prefrontal cortical parvalbumin interneurons facilitates extinction of reward-seeking behavior', *J Neurosci,* 34(10), pp. 3699-705.

816   Tierney, P. L., Degenetais, E., Thierry, A. M., Glowinski, J. and Gioanni, Y. (2004) 'Influence of
817   the hippocampus on interneurons of the rat prefrontal cortex', *Eur.J.Neurosci.,* 20(2), pp.
818   514-524.
819   Vertes, R. P. (2004) 'Differential projections of the infralimbic and prelimbic cortex in the rat',
820   *Synapse,* 51(1), pp. 32-58.
821   Vertes, R. P. (2006) 'Interactions among the medial prefrontal cortex, hippocampus and midline
822   thalamus in emotional and cognitive processing in the rat', *Neuroscience,* 142(1), pp. 1-
823   20.
824   Vidal-Gonzalez, I., Vidal-Gonzalez, B., Rauch, S. L. and Quirk, G. J. (2006) 'Microstimulation
825   reveals opposing influences of prelimbic and infralimbic cortex on the expression of
826   conditioned fear', *Learn.Mem.,* 13(6), pp. 728-733.
827   Villaruel, F. R., Lacroix, F., Sanio, C., Sparks, D. W., Chapman, C. A. and Chaudhri, N. (2017)
828   'Optogenetic Activation of the Infralimbic Cortex Suppresses the Return of Appetitive
829   Pavlovian-Conditioned Responding Following Extinction', *Cereb Cortex*, pp. 1-12.
830   Warlow, S. M., Robinson, M. J. F. and Berridge, K. C. (2017) 'Optogenetic Central Amygdala
831   Stimulation Intensifies and Narrows Motivation for Cocaine', *J Neurosci,* 37(35), pp.
832   8330-8348.
833   Wright, C. I., Beijer, A. V. and Groenewegen, H. J. (1996) 'Basal amygdaloid complex afferents
834   to the rat nucleus accumbens are compartmentally organized', *J Neurosci,* 16(5), pp.
835   1877-93.
836   Zeeb, F. D., Baarendse, P. J., Vanderschuren, L. J. and Winstanley, C. A. (2015) 'Inactivation of
837   the prelimbic or infralimbic cortex impairs decision-making in the rat gambling task',
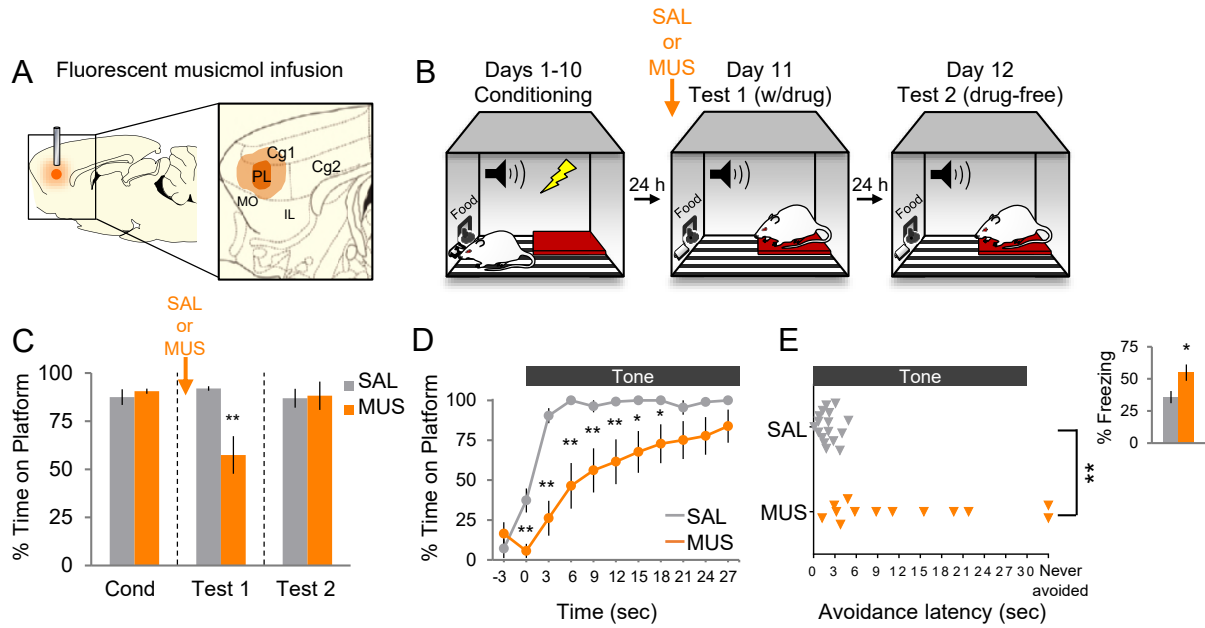838   *Psychopharmacology (Berl),* 232(24), pp. 4481-91.
839

Figure 1. Pharmacological inactivation of prelimbic cortex delays avoidance. A. Schematic of MUS infusion showing min (dark orange) and max (light orange) extent of infusion in PL. **B**. Rats were trained across 10 days to avoid a tone-signaled foot-shock by stepping onto a platform. On Day 11, rats received 2 tone presentations (without shock) 45 min after MUS infusion. On Day 12, rats received a second 2-tone test drug free. **C**. Percent time on platform during Tone 1 on Days 10, 11 (with MUS), and 12 for saline controls (SAL, n=17; grey) and MUS rats (n=13, orange). **D**. Time spent on platform in 3 sec bins (Tone 1, Test 1) revealed that MUS rats were significantly delayed in their avoidance compared to SAL controls (repeated measures ANOVA, post hoc Tukey). **E**. Latency of avoidance for each rat (Mann Whitney U test, Tone 1, Test 1). *Inset*: Effect of MUS inactivation (Tone 1, test 1) on freezing during the tone (unpaired t-test). Data are shown as mean ± SEM; *p<0.05, **p<0.01.
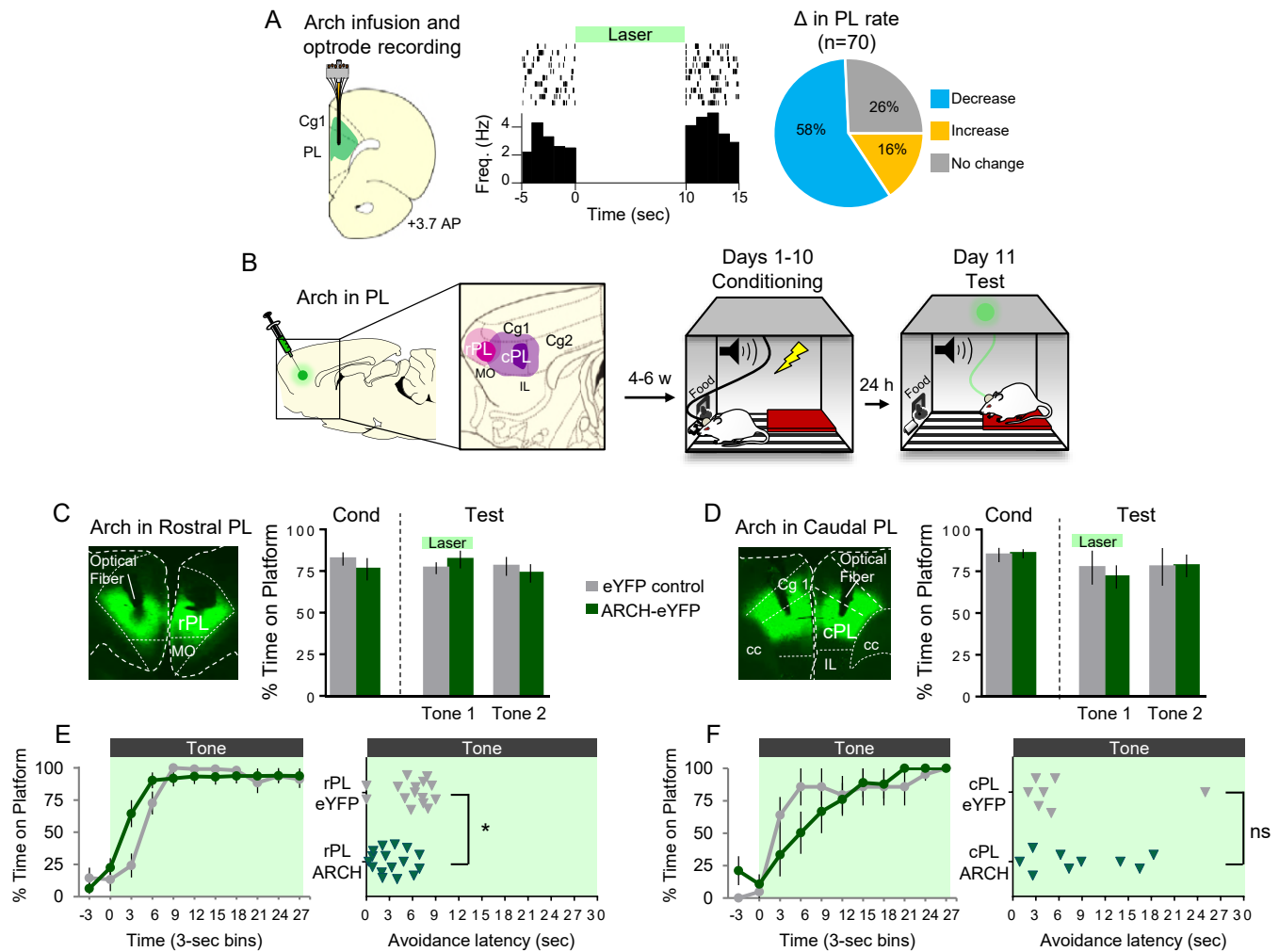
Figure 2. Optogenetic silencing of prelimbic neurons does not delay avoidance. A. *Left*: Schematic of Arch expression and optrode placement (n=2 rats). *Middle*: Rasters and peristimulus time histogram of a single PL neuron showing a decrease in firing rate during laser illumination (8-10mW, 532nm, 10s ON, 10s OFF, 10 trials). *Right*: Proportion of PL neurons that exhibited a decrease (blue, n=41), increase (gold, n=11), or no change (grey, n=18) in firing rate. **B**. Schematic of virus infusion, location of min/max expression of AAV in rPL (pink) and cPL (purple), followed by avoidance training and test. At Test, 532nm light was delivered to rPL or cPL during the entire 30-second tone presentation (Tone 1). **C**. *Left*: Micrograph of Arch expression and optical fiber placement in rPL. *Right*: Percent time on platform at Cond (Day 10, Tone 1) and Test (Day 11, Tone 1 with laser ON and Tone 2 with laser OFF) for eYFP-rPL control (n=15, grey) and Arch-rPL rats (n=17, green). **D**. *Left*: Micrograph of Arch expression and optical fiber placement in cPL. *Right*: Percent time on platform during Cond and Test for eYFP-cPL control (n=7, grey) and Arch-cPL rats (n=9, green). **E**. *Left*: Time spent on platform in 3 sec bins (Tone 1 at Test) revealed no effect of silencing rPL-Arch neurons compared to eYFP controls (repeated measures ANOVA, post hoc tukey). *Right*: Latency of avoidance for each rat (Tone 1 at Test). rPL-Arch rats showed a decrease in avoidance latency (Mann Whitney U test, p<0.05). **F**. Timeline of avoidance (left) and latency (right) for cPL-eYFP control rats and cPL-Arch rats. All data are shown as mean ± SEM; p<0.05.
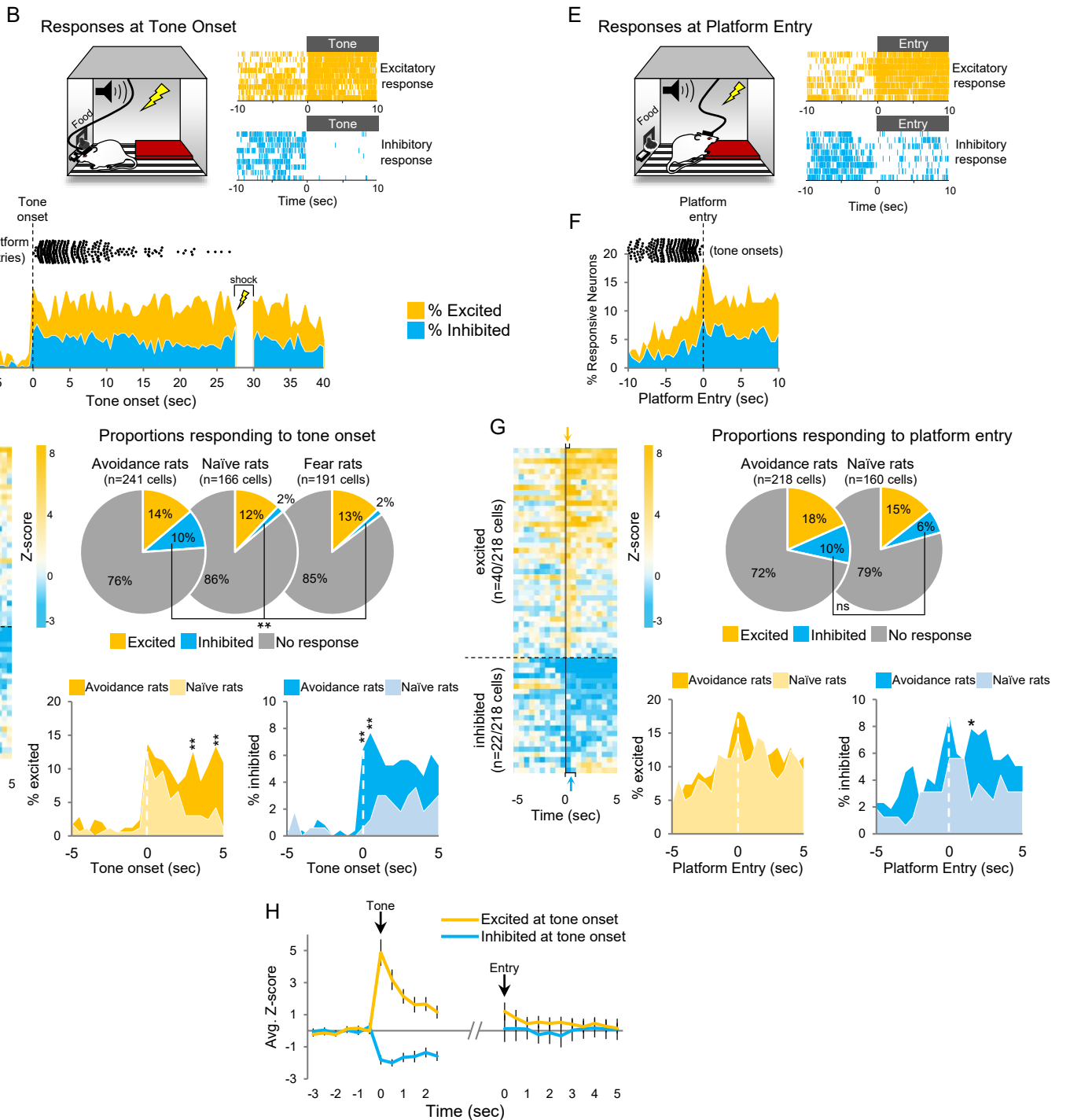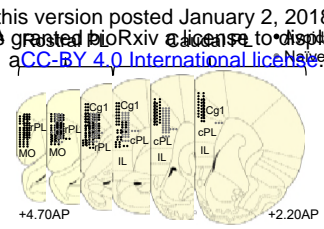
Figure 3. Initiation of avoidance is correlated with inhibition in rostral PL neurons. A. Location of recordings across PL (n=7 avoidance-trained and n=8 naïve rats). **B**. *Left*: Cartoon of rat behavior at tone onset during unit recordings. *Right*: single unit examples of an excitatory (gold rasters) and inhibitory tone response (blue rasters). Each row represents a single trial. **C**. Percentage of neurons that were excitatory (gold) or inhibitory (blue) throughout the tone. Time of platform entry (black dots), for all successful trials (n=340) in avoidance rats is indicated relative to tone onset. **D**. *Left*: Heat map of normalized responses (z-score) to tone onset (Time = 0 sec) of neurons in avoidance rats. Each row represents one neuron, bin = 0.5 sec. Arrows indicate bins used to determine criteria for excitatory (gold, first 500ms bin), or inhibitory (blue, first or second 500ms bin) tone responses. *Right:* Pie charts showing proportions of neurons that were excited, inhibited, or non-responsive at tone onset in avoidance (n = 34, 25, 182, respectively), naïve (n = 20, 3, 143, respectively), and fear conditioned rats (n = 25, 3, 163, respectively). Proportion of inhibitory responses were significantly greater in avoidance rats compared to naïve and fear rats (Chi Square test, **p<0.001). *Bottom*: Percentage of cells that were excited in avoidance (gold) or naïve (light gold) rats (left) or inhibited in avoidance (blue) or naïve (light blue) rats (right) around tone onset (Fisher exact tests). **E**. *Left*: Cartoon of rat entering platform after tone onset during unit recordings. *Right*: single unit examples of an excitatory (gold rasters) and inhibitory platform entry response (blue rasters). **F**. Percentage of neurons that were excitatory (gold) or inhibitory (blue) at platform entry. Time of tone onset (black dots), for all successful trials (n=340) in avoidance rats is indicated relative to platform entry. **G**. *Left*: Heat map of normalized responses to platform entry (Time = 0 sec) of neurons in avoidance rats. *Right*: Pie charts showing proportions of neurons that were excited, inhibited, or non-responsive at platform entry in avoidance (n = 40, 22, 156, respectively) and naïve rats (n = 23, 10, 127, respectively). *Bottom*: Percentage of cells that were excited in avoidance (gold) or naïve (light gold) rats (left) or inhibited in avoidance (blue) or naïve (light blue) rats (right) after platform entry (Fisher exact tests). **H**. Tone responsive neurons were not responsive to platform entry. All data are shown as mean ± SEM; *p<0.05, **p<0.01.
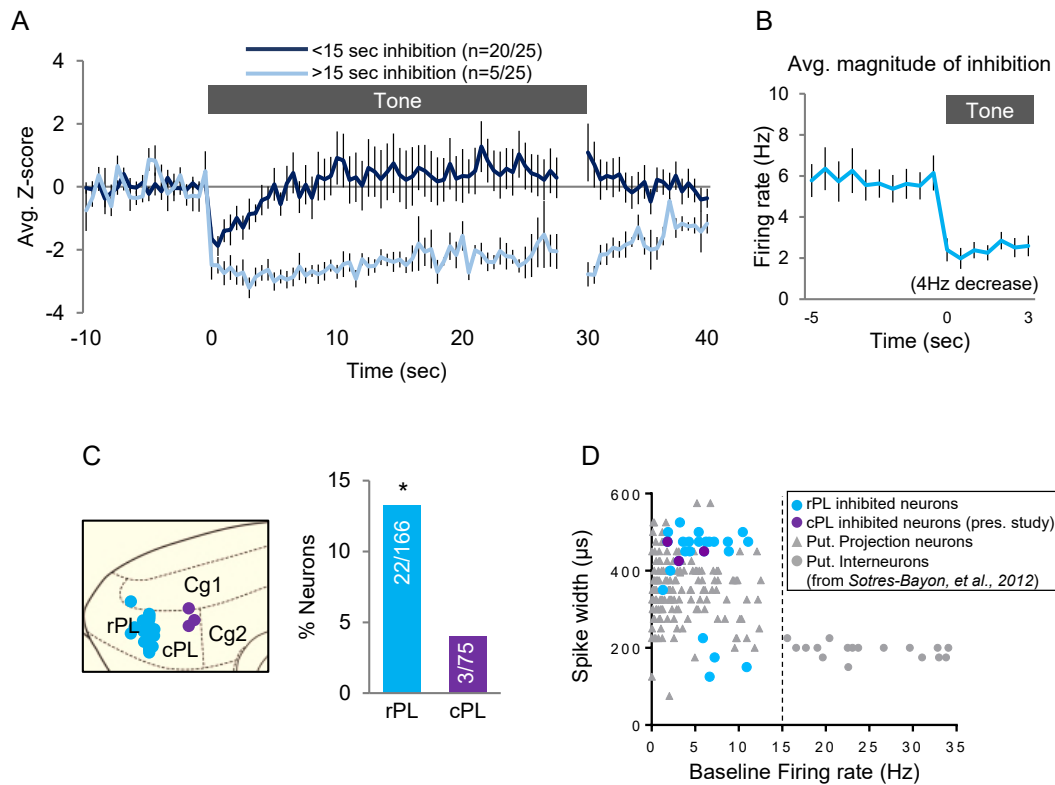
Figure 4. Characterization of inhibitory tone responsive neurons. A. Normalized firing rate of cells that were inhibited for less than 15 sec (dark blue) or more than 15 sec (light blue) after tone onset. **B**. Average inhibitory response of neurons decreased from a baseline firing rate of 5.8 Hz to 1.98 Hz at tone onset. **C**. *Left*: sagittal view of location of inhibitory tone responsive neurons in rPL (blue) or cPL (purple). *Right*: Histological analysis revealed that more inhibited neurons were located in rPL (Fisher Exact Test). **D**. Classification of PL neurons into putative projection neurons (gray triangle) or interneurons (gray circle) based on spike width and baseline firing rate (Sotres-Bayon et al, 2012). Neurons showing inhibitory responses (blue/purple, n=25) were likely projection neurons. All data are shown as mean ± SEM; *p<0.05.
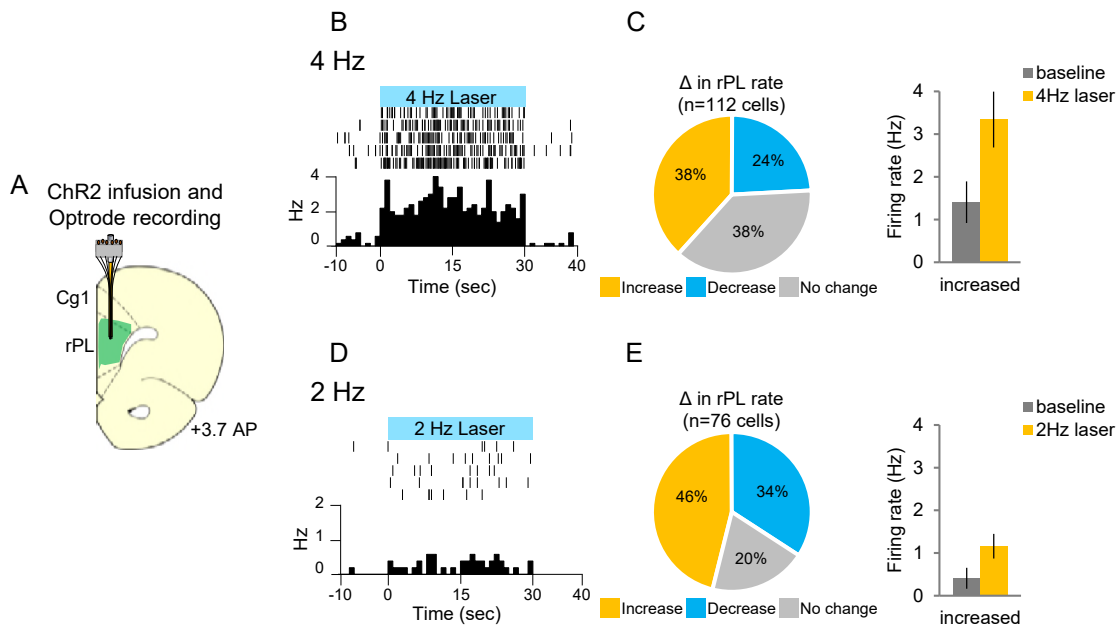
Figure 5. 4 Hz photoactivation and single unit recordings of rostral PL neurons in anesthetized rats. A. Schematic of ChR2 expression and optrode placement (n=4 rats). **B**. Rasters and peristimulus time histograms of a representative single neuron showing increased firing rate during laser illumination (8-10mW, 473nm, 30s ON, 30s OFF, 4 Hz, 5 trials). **C**. *Left*: Proportion of neurons showing an increase (gold, n=43), decrease (blue, n=27), or no change (grey, n=42) in firing rate with laser ON. *Right*: Average firing rate at baseline (dark grey) and 4 Hz photoactivation for neurons showing increased (gold) changes in firing rate. **D**. Rasters and peristimulus time histograms of a representative single neuron showing increased firing rate during laser illumination (8-10mW, 473nm, 30s ON, 30s OFF, 2 Hz, 5 trials). **E**. *Left*: Proportion of neurons showing an increase (n=35), decrease (n=26), or no change (n=15) in firing rate with laser ON. *Right*: Average firing rate at baseline, and 2 Hz photoactivation for neurons showing increased changes in firing rate. All data are shown as mean ± SEM.
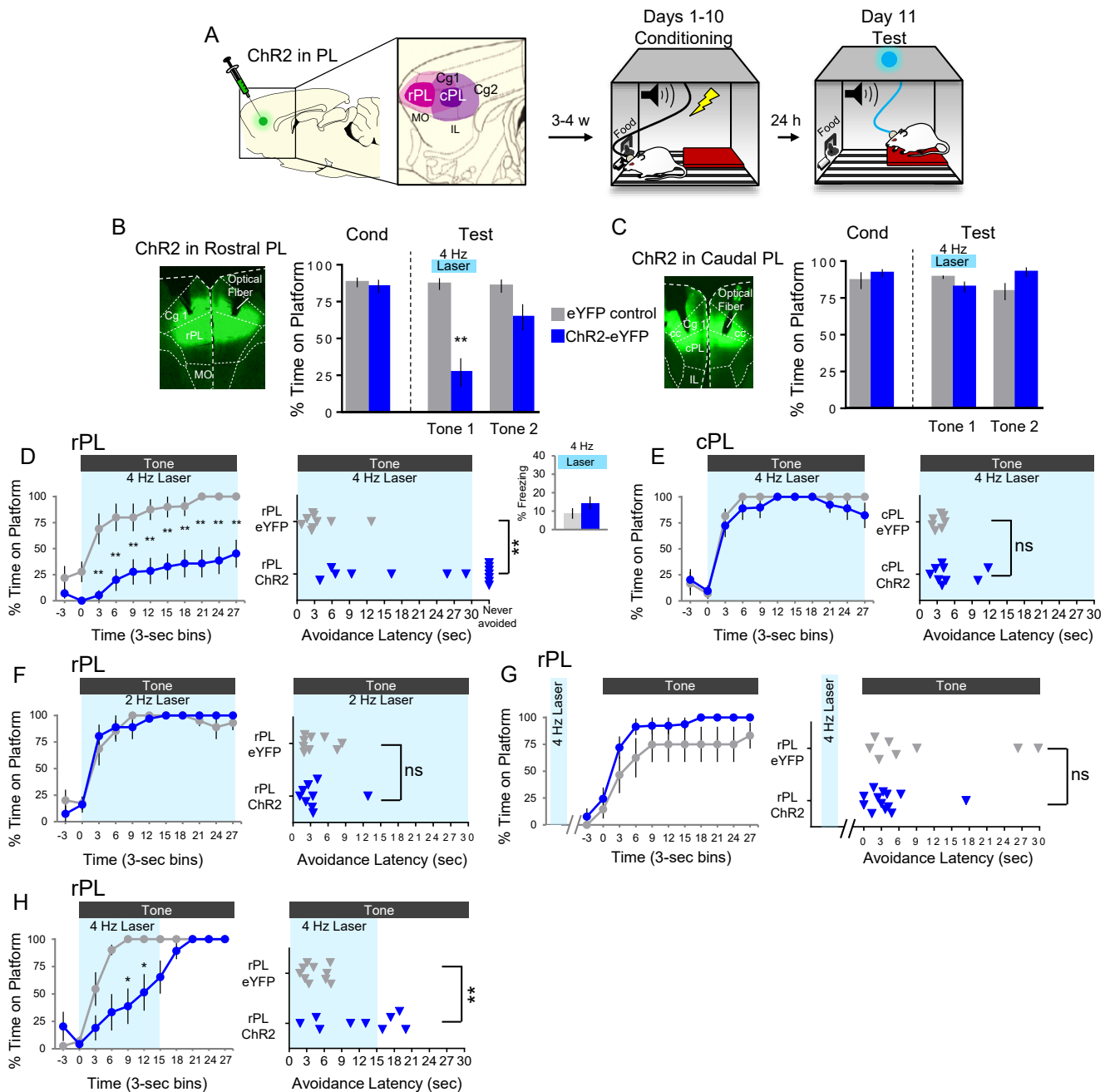
Figure 6. 4 Hz photoactivation of rostral PL neurons during the tone delays or prevents avoidance. A. Schematic of viral infusion and location of min/max spread of AAV expression in rPL (pink) and cPL (purple), followed by avoidance training and test. At Test, 473nm light was delivered to rPL or cPL during the first 30-second tone presentation (Tone 1). **B**. *Left*: Micrograph of ChR2 expression and optical fiber placement in rPL. *Right*: Percent time on platform at Cond (Day 10, Tone 1) and Test (Day 11, Tone 1 with laser ON and Tone 2 with laser OFF) for eYFP-rPL control rats (grey, n=9) and ChR2-rPL rats (blue, n=14). **C**. *Left*: Micrograph of ChR2 expression and optical fiber placement in cPL. *Right*: Percent time on platform during Cond and Test for eYFP-cPL control rats (grey, n=7) and ChR2-cPL rats (blue, n=9). **D**. *Left*: Time spent on platform in 3 sec bins (Tone 1 at Test) revealed that rPL-ChR2 rats were significantly delayed in their avoidance compared to eYFP controls (repeated measures ANOVA, post hoc tukey). *Right*: Latency of avoidance for each rat (Mann Whitney U test, Tone 1 at Test). 7/14 rats never avoided. *Inset*: 4 Hz photoactivation in rPL had no effect on freezing (Tone 1 at Test). **E**. Timeline of avoidance (left) and latency (right) for eYFP-cPL control ChR2-cPL rats revealed no effect of 4 Hz photoactivation of cPL. **F**. Timeline of avoidance (left) and latency (right) for eYFP-rPL control rats (grey, n=9) and ChR2-rPL rats (blue, n=9) revealed no effect of 2 Hz photoactivation. **G**. Timeline of avoidance (left) and latency (right) for eYFP-rPL control rats (grey, n=8) and ChR2-rPL rats (blue, n=13) revealed no effect of 4Hz photoactivation during a 30 sec ITI period. **H**. Timeline of avoidance (left) and latency (right) for eYFP-rPL control rats (grey, n=10) and ChR2-rPL rats (blue, n=9) revealed a delay in the initiation of avoidance with 4Hz photoactivation during the first 15 sec of the tone (Mann Whitney U test for time course and avoidance latency). All data are shown as mean ± SEM; *p<0.05; **p<0.01.